THE JOURNAL OF BIOLOGICAL CHEMISTRY Vol. 276, No. 47, Issue of November 23, pp. 44266–44274, 2001
Printed in U.S.A.

Identification of a Heregulin Binding Site in HER3 Extracellular Domain*

Received for publication, June 12, 2001, and in revised form, August 28, 2001
Published, JBC Papers in Press, September 12, 2001, DOI 10.1074/jbc.M105428200

Elizabeth Singer‡§, Ralf Landgraf¶, Tom Horan‖, Dennis Slamon¶, and David Eisenberg‡§**

From the ‡Department of Chemistry and Biochemistry, UCLA, Los Angeles, California 90095-1569, §Howard Hughes Medical Institute, UCLA-Department of Energy Laboratory of Structural Biology and Molecular Medicine, Los Angeles, California 90095-1570, ‖Amgen Inc., Amgen Center, Thousand Oaks, California 91320, and ¶Division of Hematology-Oncology, Department of Medicine, UCLA School of Medicine, Los Angeles, California 90095

HER3 (also known as c-Erb-b3) is a type I receptor tyrosine kinase similar in sequence to the epidermal growth factor (EGF) receptor. The extracellular segment of this transmembrane receptor contains four domains. Domains I and II are similar in sequence to domains III and IV, respectively, and domains II and IV are cysteine-rich. We show that the EGF-like domain of heregulin (hrg) binds to domains I and II of HER3, in contrast to the EGF receptor, for which prior studies have shown that a construct consisting of domains III and portions of domain IV binds EGF. Next, we identified a putative hrg binding site by limited proteolysis of the recombinant extracellular domains of HER3 (HER3-ECD$^{I–IV}$) in both the presence and absence of hrg. In the absence of hrg, HER3-ECD$^{I–IV}$ is cleaved after position Tyr^{50}, near the beginning of domain I. Binding of hrg to HER3-ECD$^{I–IV}$ fully protects position Tyr^{50} from proteolysis. To confirm that domain I contains a hrg binding site, we expressed domains I and II (HER3-ECD^{I-II}) and find that it binds hrg with 68 nM affinity. These data suggest that domains I and II of HER3-ECD$^{I–IV}$ act as a functional unit in folding and binding of hrg. Thus, our biochemical findings reinforce the structural hypothesis of others that HER3-ECD$^{I–IV}$ is similar to the insulin-like growth factor-1 receptor (IGF-1R), as follows: 1) The protected cleavage site in HER3-ECD$^{I–IV}$ corresponds to a binding footprint in domain I of IGF-1R; 2) HER3-ECD^{I-II} binds hrg with a 68 nM dissociation constant, supporting the hypothesis that domain I is involved in ligand binding; and 3) the large accessible surface area (1749 Å) of domain L1 of IGF-1R that is buried by domain S1, as well as the presence of conserved contacts in this interface of type 1 RTKs, suggests that domains L1 and S1 of IGF-1R function as a unit as observed for HER3-ECD^{I-II}. Our results are consistent with the proposal that HER3 has a structure similar to IGF-1R and binds ligand at a site in corresponding domains.

Human epidermal growth factor receptor 3 (HER3)[1] (1) is a member of the type I receptor tyrosine kinase (RTK) family, which also includes EGFR, HER2/*neu*, and HER4 (2–4). HER3 forms heterodimers with other members of the type I RTK family, including the HER2/*neu* receptor (5–8). The HER2/*neu* receptor is amplified and overexpressed in 25–30% of human breast and 8–11% of human ovarian cancers. This overexpression correlates with increased morbidity and mortality, and there is evidence that the overexpressed HER2 receptor leads to aggressive malignancies (9–12). The HER2/HER3 heterodimer forms a high affinity heregulin receptor with tyrosine kinase activity. Heregulin binding to cells that display the HER2/HER3 heterodimer causes a mitogenic response both *in vitro* and *in vivo*, so understanding this interaction is of medical importance (13).

The type I RTKs contain four extracellular domains, a single hydrophobic transmembrane segment, and a cytoplasmic tyrosine kinase domain (14). HER2/*neu* is a very active tyrosine kinase, but cells expressing HER2/*neu* alone, and not other members of the EGFR family, fail to bind heregulin. Conversely, the HER3 receptor binds heregulin but has low tyrosine kinase activity (15, 16). As mentioned above, the HER2/HER3 heterodimer is a high affinity heregulin binding complex with signaling activity through the HER-2 kinase domain. To date, the domains of HER3 involved in ligand binding and heterodimerization have not been identified.

Thus far, the high carbohydrate content (17) and the relatively large size (~180 kDa) of the receptors in the EGFR family have hindered structural analysis by x-ray crystallography and NMR, so other methods have been sought to illuminate the structure and function of HER3. The extracellular domains (ECDs) of the type I RTKs have been divided into four domains: I, II, III, and IV, based on sequence analysis (18). Domains II and IV are cysteine-rich and are similar in sequence. Domains I and III also have sequence similarity (18, 19). Little is known about the specific function of each domain except in EGFR, where several lines of evidence suggest that the major determinants for EGF binding lie in domain III. These lines of evidence include the following: 1) the exchange of domain III in chicken EGFR for domain III from human EGFR confers binding of human EGF (20, 21); 2) monoclonal antibodies that recognize residues in domain III prevent EGF binding to EGFR

* The UCLA Protein Microsequencing Facility is partially supported by NCI, National Institutes of Health (NIH), Cancer Center Support Grant CA 16042. Financial support was provided by NIH and the Revlon/UCLA Women's Cancer Research Program. The costs of publication of this article were defrayed in part by the payment of page charges. This article must therefore be hereby marked "*advertisement*" in accordance with 18 U.S.C. Section 1734 solely to indicate this fact.

** To whom correspondence should be addressed: UCLA-Department of Energy Laboratory of Structural Biology and Molecular Medicine, Molecular Biology Institute, Box 951750, Los Angeles, CA 90095-1570. Tel.: 310-825-3754; Fax: 310-206-3914; E-mail: david@mbi.ucla.edu.

[1] The abbreviations used are: HER, human epidermal growth factor receptor; ECD, extracellular domain; EGF, epidermal growth factor; EGFR, epidermal growth factor receptor; hrg, 60-residue EGF-like domain of human heregulin β1; IGF-1R, insulin growth factor-1 receptor; IR, insulin receptor; NA_5-hrg, binding-deficient hrg mutant; PBS, phosphate-buffered saline; RTK, receptor tyrosine kinase; trx-hrg, thioredoxin-heregulin fusion; β-ME, β-mercaptoethanol; PAGE, polyacrylamide gel electrophoresis; BSA, bovine serum albumin; MALDI, matrix-assisted laser desorption/ionization; SPR, surface plasmon resonance; MES, 4-morpholineethanesulfonic acid.

(22); 3) cross-linking of EGF to EGFR identified residues in domain III (23, 24); and 4) limited proteolysis of the ECD of EGFR produced a fragment that encompassed domain III, which bound transforming growth factor, with the observation that binding could be enhanced by including portions of domain IV (25). Additional studies from cross-linking experiments indicated that bound EGF is also close to tyrosine 101 in domain I of murine EGFR (26). Taken together, these experimental results suggest that domain I and III are close to the ligand-binding region in EGFR and that domain III contributes most of the binding.

HER3 and EGFR have relatively high sequence identity (45% identity in the ECD) and belong to the same family of type 1 tyrosine kinase receptors; however, they bind a different subset of ligands and differ in preference for heterodimerization *versus* homodimerization (8, 27–29). In this study, we have carried out a limited proteolysis of the extracellular domains of HER3 in an attempt to identify regions in the four extracellular domains of HER3 (HER3-ECD$^{I–IV}$) that are essential for heregulin binding.

EXPERIMENTAL PROCEDURES

Materials—Soluble extracellular domains of recombinant HER3 (HER3-ECD$^{I–IV}$) were purified from Chinese hamster ovary cells by the procedure of Kita *et al.* (30). The 60-residue EGF-like domain of human heregulin β1 (residues 177–237) (hrg), the binding-deficient heregulin mutant (NA_5-hrg), and the thioredoxin-heregulin fusion with a C-terminal His and S-tag (trx-hrg) were generated and purified as described elsewhere (31). EGF was purchased from Sigma. Trypsin was purchased from Life Technologies, Inc. (catalog number 15400–013 and lot numbers 12P6334 and 1023241) and Sigma (catalog number T-1426 and lot number 70K7661), which had been treated with tosylamide-2-phenylethylchloromethyl ketone to remove chymotrypsin.

Proteolytic Digest—5.0 μl of (HER3-ECD$^{I–IV}$) at 2.3 mg/ml in storage buffer (20 mM sodium acetate pH 5.5 and 40 mM sodium chloride), 10 μl of phosphate-buffered saline (PBS): 136 mM NaCl, 2.68 mM KCl, 9.289 mM Na_2HPO_4, 1.969 mM KH_2PO_4), and 3.0 μl of trypsin (Life Technologies, Inc.; catalog number 15400-013 and lot number 12P6334) at 5.0 mg/ml in 5.0 mM EDTA and 150 mM sodium chloride were incubated at 37 °C for 1 h. Digestion was stopped by adding phenylmethylsulfonyl fluoride at a final concentration of 1.0 mM. 5.0 μl of the digested sample were added to 5.0 μl of 2× SDS-PAGE sample buffer with and without 1.0 mM β-mercaptoethanol (β-ME). These samples were then analyzed by SDS-PAGE on a 10–15% Phast gel (Amersham Pharmacia Biotech) and visualized by Coomassie staining. Different sources of trypsin were compared, but the best results were obtained with tissue culture grade trypsin from Life Technologies, Inc., which may contain other proteases.

HER3-ECD$^{I–IV}$ was titrated with hrg to determine the minimum amount required for complete protection of HER3-ECD$^{I–IV}$ from proteolysis. Hrg in PBS was incubated with HER3-ECD$^{I–IV}$ for 30 min at room temperature, followed by trypsin as described above. The final concentration of hrg in the digest ranged from 1.7 to 17 μM with a constant HER3-ECD$^{I–IV}$ concentration of 7.7 μM. These reaction mixtures were analyzed by reducing SDS-PAGE as described above. The proteolytic digest was repeated with NA_5-hrg and EGF using a molar ratio of 1:1.

Heregulin Binding by a Gel Mobility Shift Assay—HER3-ECD$^{I–IV}$ (1.4 μl) in storage buffer was incubated with 9.6 μl of hrg (6.6 μM in PBS) for 30 min at room temperature. 4.0-μl aliquots of this mixture were run on a 10–15% Phast gel under native conditions. This assay was repeated for NA_5-hrg, EGF, and proteolyzed HER3-ECD$^{I–IV}$ under the same conditions.

"Pull-down" Assay Using Immobilized Trx-hrg—The ability of proteolyzed HER3-ECD$^{I–IV}$ to bind hrg was analyzed by a pull-down assay. S-protein agarose (0.5 ml) (Novagen) was spun down and resuspended three times in PBS. Aliquots of 100 μl were spun again, and trx-hrg (600 nM) and bovine serum albumin (BSA) (1 mg/ml) were added to the resin. After incubating 15 min at 4 °C, the resin was washed five times with PBS, and blocked again with BSA. The following samples were added to each aliquot of resin: HER3-ECD$^{I–IV}$, proteolyzed HER3-ECD$^{I–IV}$, HER3-ECD$^{I–IV}$ protected by hrg during proteolysis, and HER3-ECD$^{I–IV}$ incubated with trypsin deactivated with 1 mM phenylmethylsulfonyl fluoride prior to the proteolysis reaction. HER3-ECD$^{I–IV}$ was at 600 nM. BSA (1 mg/ml) was also added to each aliquot. Following a 15-min incubation at 4 °C, the resin was spun down and resuspended three times in PBS. Each aliquot of resin was then resuspended in PBS containing 1 μM hrg or PBS. After a 1-min incubation at 4 °C, the samples were spun down, and the supernatant was diluted with 2× SDS-PAGE sample buffer containing 1.0 mM β-ME. Each aliquot of resin was then resuspended in SDS-PAGE sample buffer. The samples were analyzed by SDS-PAGE on a 4–15% polyacrylamide gradient gel (Bio-Rad) and visualized by Western blotting and chemiluminescence using a polyclonal antibody directed against the HER3-ECD (E38530; Transduction Laboratories, Lexington, KY) followed by incubation with a secondary antibody conjugated to horseradish peroxidase (Invitrogen).

The ability of HER3-ECD^{I-II} to bind hrg was also evaluated in the pull-down assay in the same way, with the following exceptions. HER3-ECD^{I-II} (600 nM) was added to the trx-hrx and control resins, and the individual samples were resuspended in the various competing ligands indicated in Fig. 5. HER3-ECD^{I-II} was visualized by Western blotting and chemiluminescence using a monoclonal antibody directed against the V-5 epitope conjugated to horseradish peroxidase (Invitrogen).

Identification of the Digested Fragments—Proteolytically digested HER3-ECD$^{I–IV}$ was diluted with sample buffer containing β-ME and run on a 4–15% polyacrylamide gradient gel (Bio-Rad) as described above. The samples were then transferred to a polyvinylidene difluoride membrane, and the fragments were visualized by Ponceau stain. Edman sequencing of excised bands was performed in the UCLA Protein Microsequencing Facility using a Porton-Beckman Gas Phase Sequencer, and the first 10 residues of each fragment were identified. HER3-ECD$^{I–IV}$ was proteolyzed in the presence of an equimolar amount of an antibody against the C-terminal V5 epitope for 30, 60, and 120 min. The C-terminal fragment was identified by Western blotting using an antibody against the C-terminal V5 epitope (Invitrogen).

Amino Acid Analysis—The molar concentrations of HER3-ECD$^{I–IV}$, hrg, and NA_5-hrg were determined by amino acid analysis at the UCLA Protein Microsequencing Facility. The samples were hydrolyzed in 6 N HCl at 110 °C for 18 h under a vacuum in a nitrogen atmosphere. The hydrolysate was visualized with phenylisothiocyanate. The phenylisothiocyanate amino acids were analyzed on a reverse phase column (Novapak) using a sodium acetate-acetonitrile gradient (32, 33).

Matrix-assisted Laser Desorption Ionization (MALDI) Mass Spectrometry—We used MALDI time-of-flight mass spectrometry to measure the molecular mass of proteolyzed HER3-ECD$^{I–IV}$ and HER3-ECD^{I-II}. The mass spectrometry was performed on a Voyager RP machine (PerCeptive Biosystems, Framingham, Massachusetts) with BSA as an internal standard. 0.3 μl of HER3-ECD$^{I–IV}$ (2.3 mg/ml) in 20 mM sodium acetate pH 5.5, 40 mM sodium chloride was mixed with 0.5 μl of 10 mg/ml sinapinic acid in 70% acetonitrile, 0.1% trifluoracetate and dried on the MALDI plate. The digests (plus and minus hrg) of HER3-ECD$^{I–IV}$ were prepared in the same way, except that the sample was taken directly from the digest reaction after 1 h of incubation time. The digests were run under oxidizing and reducing conditions. The digests were reduced by the addition of 1 mM dithiothreitol prior to mixing the sample with the matrix. The molecular mass of HER3-ECD^{I-II} (12 μM) in PBS was measured under the same conditions.

Sequence Alignments and Surface Area Calculations—An initial multiple sequence alignment was performed with the GCG program Pileup (Wisconsin Package, SeqLab, SeqWeb) using the Blossum 62 matrix (34). Empirical observations of the N terminus were used in conjunction with the initial alignment to produce a final alignment. We used the GCG program Bestfit (Wisconsin Package, SeqLab, SeqWeb) (35) to find the segment of greatest similarity between two sequences. The amount of solvent-exposed surface area of domain L1 that is buried by domain S1 of IGF-1R was calculated using the GCG program Areaimol (36, 37).

Cloning and Expression of HER3-ECD^{I-II}—The HER3 cDNA was amplified from the pJTH3 plasmid provided by Amgen, using the N-terminal primer (CTA GTC TCT AGA TCC GAG GTG GGC AAC TCT) and C-terminal primer (TAC CGA TCT AGA TTT CGG ACA GAG ACC CCC). Following amplification, HER3-ECD^{I-II} (residues 20–329) was cloned into the *Bgl*II and *Xba*I site of the pMT/BiP/V5-His-A expression vector (Invitrogen, Carlsbad, CA). This vector contains an N-terminal *Drosophila* leader sequence and C-terminal His tag and V5 epitope tags. S2 cells were co-transfected with the vector containing HER3-ECD^{I-II} and the pCoHYGRO vector (Invitrogen), which provides hygromycin resistance. We obtained a stable cell line after 3 weeks of selection with 300 μg/ml hygromycin (Invitrogen). Five liters of S2 medium (Sigma) with 1% fetal bovine serum were inoculated with S2 cells and grown to a cell density of 5×10^6 in a spinner flask (Bellco) and then induced for 3 days at room temperature with 500 μM $CuSO_4$. HER3-

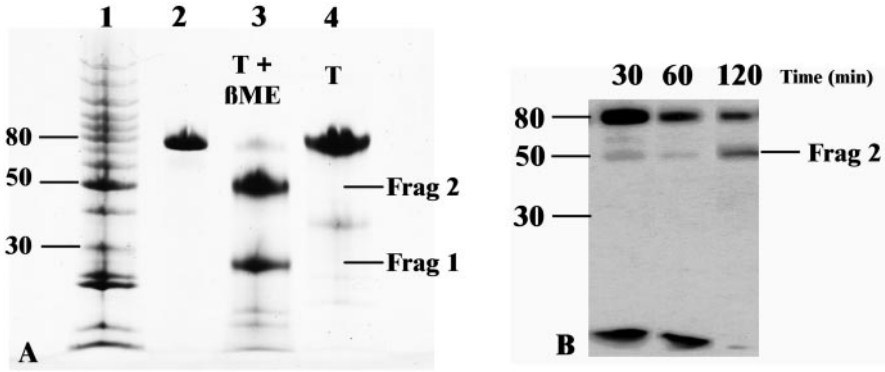

FIG. 1. *A*, limited proteolysis of HER3-ECD$^{I–IV}$ generates two detectable fragments, which remain associated under oxidizing conditions. HER3-ECD$^{I–IV}$ was digested in the presence of trypsin (*T*) and analyzed in the Phast gel in the presence of the reducing agent β-ME. The proteolytic digest of HER3-ECD$^{I–IV}$ was analyzed on an SDS-PAGE Phast gel (10–15%) in the absence (*lane 4*) and the presence (*lane 3*) of the reducing agent β-ME. Nonproteolyzed HER3-ECD$^{I–IV}$ in the presence of β-ME is shown in *lane 2*. The two fragments in proteolyzed HER3-ECD$^{I–IV}$ remain linked by one or more disulfide bridges. *B*, a V5 antibody protects HER3-ECD$^{I–IV}$ from cleavage at the C terminus. When HER3-ECD$^{I–IV}$ is proteolyzed in the absence of the V5 antibody, the C terminus is digested and could not be visualized when probed for the V5 epitope. This gel shows HER3-ECD$^{I–IV}$ proteolyzed for the time indicated in the presence of an antibody against the V5 epitope tag, analyzed on a 4–15% polyacrylamide gradient gel, and transferred to a polyvinylidene difluoride membrane. The C-terminal fragment was identified by Western blotting using an antibody against the C-terminal V5 epitope. The V5 antibody protects the C terminus against proteolytic cleavage and shows that fragment 2 is the C-terminal fragment.

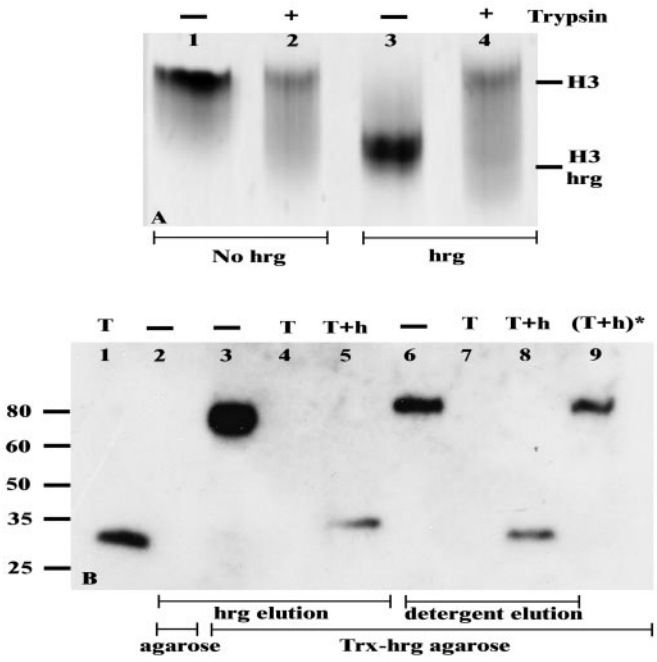

FIG. 2. *A*, nonproteolyzed HER3-ECD$^{I–IV}$ binds hrg, but proteolyzed HER3-ECD$^{I–IV}$ does not. The presence (+) or absence (−) of tryspin in the proteolytic digest is indicated *above* the *lanes*. HER3-ECD$^{I–IV}$ was analyzed on a native Phast gel (10–15%) in the absence (*lane 1*) and presence (*lane 3*) of equimolar hrg. Proteolyzed HER3-ECD$^{I–IV}$ was also analyzed in the absence (*lane 2*) and presence (*lane 4*) of hrg. Formation of a hrg-HER3-ECD$^{I–IV}$ complex is observed with the nonproteolyzed HER3-ECD$^{I–IV}$ but not with the proteolyzed HER3-ECD$^{I–IV}$. *B*, nonproteolyzed HER3-ECD$^{I–IV}$ is eluted by hrg in a pull-down assay, but proteolyzed HER3-ECD is not. HER3-ECD$^{I–IV}$ was applied untreated (−) or digested in the absence (*T*) or presence of hrg (*T* + *h*) to agarose-bound hrg. HER3-ECD$^{I–IV}$ was detected with an antibody with an epitope in fragment 1. HER3-ECD$^{I–IV}$ was bound to immobilized hrg and could be eluted with free hrg (*lane 3*) and detergent (*lane 6*), but proteolyzed HER3-ECD$^{I–IV}$ could not be eluted with hrg (*lane 4*) or detergent (*lanes 7*). HER3-ECD$^{I–IV}$ that was protected by hrg during proteolytic digestion could be recovered by both hrg (*lane 5*) and detergent (*lane 8*). Trypsin that was treated with phenylmethylsulfonyl fluoride prior to addition to the digestion reaction (*) did abolish hrg binding by HER3-ECD$^{I–IV}$, which could then be recovered by hrg (*lane 9*). This demonstrates that proteolyzed HER3-ECD$^{I–IV}$ does not bind hrg.

ECD^{I-II} was secreted to the medium. We used an ammonium sulfate cut (80%, w/v) to precipitate the protein from the medium. The pellet was resolubilized in 20 mM Tris, pH 7.9, 1.5 M NaCl, and 0.1% Tween 20. The solution was dialyzed into 20 mM Tris, pH 7.9, 0.5 M NaCl, and 5 mM imidazole and then purified on a 5-ml Amersham Pharmacia Biotech "HITRAP Chelating" column (Amersham Pharmacia Biotech), loaded with $NiSO_4$. Following elution from the column, the protein was dialyzed into 20 mM sodium potassium phosphate, pH 10. The protein was loaded onto an anion exchange column (Bio-Rad), and pure HER3-ECD^{I-II} was collected from the flow-through.

Multiangle Light Scattering of HER3-ECD^{I-II}—Size exclusion chromatography was performed using a TosoHaas G3000SWXL column, followed by light scattering on a miniDAWN three-angle light-scattering instrument (Wyatt Technologies, Santa Barbara, CA). Data analysis was carried out using ASTRA software. HER3-ECD^{I-II} (112 μM) in 20 mM Hepes, pH 7.5, was injected onto the column at a flow rate of 0.4 ml/min. The refractive index increment (d*n*/d*c*) for the protein portion of the HER3-ECD^{I-II} in this buffer was assumed to be equal to that of monomeric BSA (Sigma) (d*n*/d*c* = 0.181 cm^3/g). The carbohydrate d*n*/d*c* contribution was estimated to be 0.157 cm^3/g and was integrated into the final d*n*/d*c* (0.180 cm^3/g) proportionally. Calculated extinction coefficients uncorrected for folding effect were used. The error to noise in the light scatter data is about ±3%. An error in the assumed extinction coefficient would result in a proportional error in the calculated molecular mass.

Ultracentrifugation of HER3-ECD^{I-II}—Sedimentation equilibrium was performed at 4 °C in a Beckman Optima XL-A analytical ultracentrifuge using absorption optics at 280 nm. A 12-mm path length six-sector cell was used to measure protein samples at initial A_{280} values of 0.15, 0.35, and 0.75. All samples were in PBS. Sedimentation equilibrium profiles were measured at 12,000 and 15,000 rpm. The data were initially fitted with a nonlinear least-squares exponential fit for a single ideal species using Origin (version 3.01). Since no concentration or speed dependence of the molecular weight was apparent, the Beckman global analysis software (the "multifit" option of the above mentioned software) was used to analyze all six scans simultaneously. A partial specific volume of 0.712 calculated from the amino acid composition and corrected to 4 °C was used (38, 39).

Surface Plasmon Resonance Measurement of Binding between HER3-ECD^{I-II} and the EGF-like Domain of Heregulin—Trx-hrg (13 μM) in MES buffer (100 mM pH 6.0) was immobilized on a BIAcore CM5 chip using standard *N*-hydroxysuccinimide/1-ethyl-3-(3-dimethylaminopropyl)carbodiimide amine-coupling chemistry. The surface of the chip was blocked with ethanolamine and could be regenerated with 5.0 M NaCl and washes with running buffer (PBS + surfactant). HER3-ECD^{I-II} (filtered through a 0.1-μm filter unit (Millipore, Bedford, MA)) in running buffer was applied to the chip at various concentrations (in triplicate) to determine the dissociation constant. Data were analyzed with the BIAevaluation software. Competition experiments were carried out using hrg at an equimolar concentration to HER3-ECD^{I-II}.

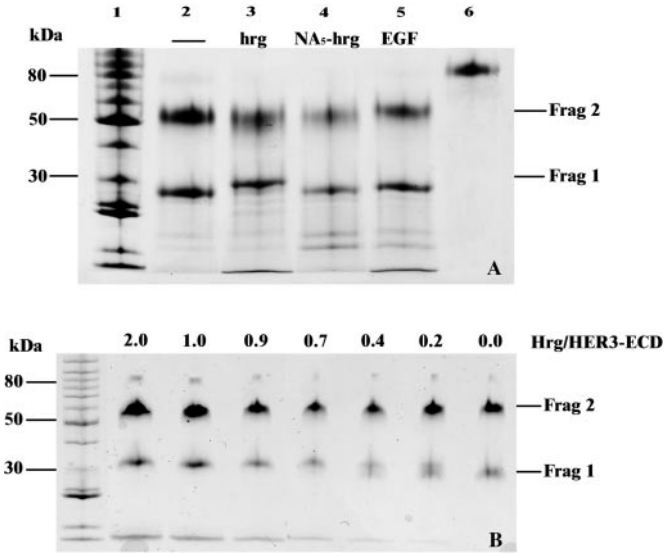

FIG. 3. *A*, limited proteolysis of HER3-ECD$^{I–IV}$ in the presence of hrg generates a different cleavage pattern than in the absence of hrg when analyzed on an SDS-PAGE Phast gel (10–15%) under reducing conditions. HER3-ECD$^{I–IV}$ was proteolyzed in the absence of ligand (−) and in the presence of hrg, NA_5-hrg, and EGF, as indicated *above* the *lanes*. Limited proteolysis of HER3-ECD$^{I–IV}$ generates two fragments: one at an apparent molecular mass of 24.2 kDa (fragment 1) and another at 54.1 kDa (fragment 2). In the presence of NA_5-hrg (*lane 4*) and EGF (*lane 5*), fragment 1 appears to be identical to fragment 1 in the absence of hrg (*lane 2*), whereas in the presence of wild type hrg (*lane 3*), fragment 1 appears to have a slightly higher molecular mass. The digest of HER3-ECD$^{I–IV}$ in the presence of a binding-competent hrg generates a different cleavage pattern than in its absence. Apparently, the cleavage that generates fragment 1 can be protected by hrg and is due to a specific interaction between hrg and HER3-ECD$^{I–IV}$. *B*, the minimum amount of hrg required to produce a change in the molecular weight of fragment 1 in the SDS gel was determined by varying the molar ratio of hrg to HER3-ECD$^{I–IV}$. The ratio of hrg to HER3-ECD$^{I–IV}$ was varied from 2.0 to 0 (*lanes 2–8*), as indicated *above* the *lanes*. A change in the molecular weight of fragment 1 was observed when the molar ratio of hrg to HER3-ECD$^{I–IV}$ was between 0.9:1 and 1:1. Complete protection of HER3-ECD$^{I–IV}$ by hrg was observed at an approximately 1:1 ratio of hrg to HER3-ECD$^{I–IV}$.

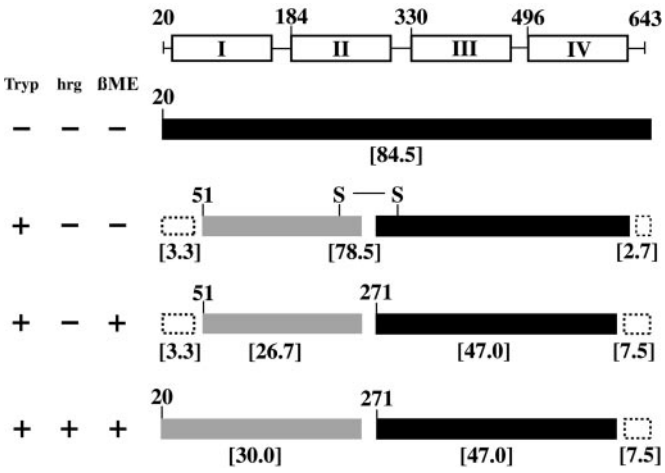

FIG. 4. **Domain organization and proteolytic cleavage sites of HER3-ECD$^{I–IV}$.** The extracellular region of HER3 contains domains I, II, III, and IV. Sequence positions are indicated at the start of each domain. The beginning of HER3-ECD$^{I–IV}$ at position 20 refers to the start of mature HER3-ECD$^{I–IV}$ after cleavage of the leader sequence. The various digests that were analyzed are shown to the *left*: the digest of HER3-ECD$^{I–IV}$ in the presence (+) and absence (−) of hrg and mass spectrometry of the oxidized (−*βME*) and reduced (+*βME*) forms of the digest. The position of the cleavage site as determined by N-terminal sequencing is indicated at the start of each fragment. Fragment 1 is indicated by a *gray bar*, and fragment 2 is represented by a *black bar*. *Numbers* in *brackets* are mass estimates in kDa as determined by mass spectrometry. *S–S* indicates that the two fragments are held together by a disulfide bond. The exact position of the cleavage at the C terminus is unknown, and this is indicated by a *dashed bar*. The postulated mass of the missing fragments is indicated in *brackets below* the *fragments* with *dashed lines*. In summary, hrg protects HER3-ECD from cleavage at position 50 but not at any other site.

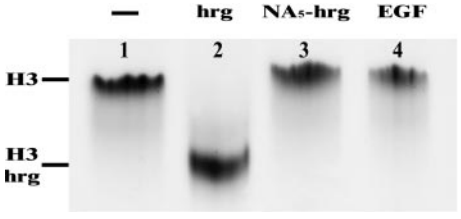

FIG. 5. **HER3-ECD$^{I–IV}$ binds hrg but not EGF or the binding-deficient NA_5-hrg.** HER3-ECD$^{I–IV}$ was analyzed on a native Phast gel (10–15%) in the absence of hrg (*lane 1*) and in the presence of hrg (*lane 2*), NA_5-hrg (*lane 3*), and EGF (*lane 4*). The ligands were used at a 1:1 ratio of hrg to HER3-ECD$^{I–IV}$. A complete shift is observed in the presence of hrg, and no shift is apparent in NA_5-hrg or EGF.

RESULTS

Proteolysis of HER3-ECD$^{I–IV}$ Results in Two Primary Fragments That Remain Associated under Oxidizing Conditions—First, we digested HER3-ECD$^{I–IV}$ to learn if limited proteolysis leads to a fragment still capable of binding hrg. This results in two principal fragments (Fig. 1*A*, *lane 3*) with apparent molecular masses of 24 kDa (fragment 1) and 54 kDa (fragment 2), compared with an apparent molecular mass for the nonproteolyzed HER3-ECD$^{I–IV}$ of 80 kDa. Gel electrophoresis of the proteolyzed HER3-ECD$^{I–IV}$ in the absence of a reducing agent shows that the two fragments remain linked by disulfide bonds (Fig. 1*A*, *lane 4*). Fragment 2 was identified as the C-terminal fragment by Western blot using the V5 C-terminal epitope-tagged HER3-ECD$^{I–IV}$ (Fig. 1*B*).

Proteolytic Cleavage of HER3-ECD$^{I–IV}$ Abolishes Heregulin Binding—To determine the effects of cleavage of HER3-ECD$^{I–IV}$ on its ability to bind hrg, a gel mobility shift assay was performed. In a native gel analysis, proteolyzed HER3-ECD$^{I–IV}$ (Fig. 2*A*, *lane 2*) shows an electrophoretic mobility similar to the nonproteolyzed HER3-ECD$^{I–IV}$ (Fig. 2*A*, *lane 1*). The nonproteolyzed HER3-ECD$^{I–IV}$ shows a discrete shift in the presence of a 1:1 molar ratio of hrg to HER3-ECD$^{I–IV}$ (Fig. 2*A*, *lane 3*). The proteolyzed HER3-ECD$^{I–IV}$ does not shift its gel position in the presence of hrg (Fig. 2*A*, *lane 4*). This finding suggests that the two disulfide-linked fragments, generated by proteolytic digestion (Fig. 1*A*, *lane 4*) do not bind hrg.

To check whether the proteolyzed HER3-ECD$^{I–IV}$ binds hrg, we used a pull-down assay under physiological salt conditions. In this analysis, we measured the HER3-ECD$^{I–IV}$ and proteolyzed HER3-ECD$^{I–IV}$ that could be dissociated from immobilized thioredoxin-heregulin (trx-hrg) by the addition of hrg. Using trx-hrg-coupled S-protein agarose, HER3-ECD$^{I–IV}$ was eluted with hrg (Fig. 2*B*, *lane 3*). No proteolyzed HER3-ECD$^{I–IV}$ could be recovered by either elution with hrg (Fig. 2*B*, *lane 4*) or detergent (Fig. 2*B*, *lane 7*). However, HER3-ECD$^{I–IV}$ that was protected by hrg during proteolytic digestion could be recovered by detergent and competition with hrg (Fig. 2*B*, *lanes 5* and *8*). In addition, a trypsin preparation that was treated with phenylmethylsulfonyl fluoride prior to the addition to the digestion reaction did not abolish hrg binding by HER3-ECD$^{I–IV}$ (Fig. 2*B*, *lane 9*). Based on these results, we conclude that the proteolyzed HER3-ECD$^{I–IV}$ does not bind hrg.

Heregulin Protects HER3-ECD$^{I–IV}$ from Proteolytic Cleavage—The observation that proteolytic cleavage destroys the binding of HER3-ECD$^{I–IV}$ to hrg suggests that cleavage occurs at or near the binding site. This led us to investigate the

proteolysis of HER3-ECD$^{I–IV}$ in the presence of hrg. The digestion of HER3-ECD$^{I–IV}$ in the presence of a molar excess of hrg (Fig. 3*A*, *lane 3*) produces a different cleavage pattern than in the absence of hrg (Fig. 3*A*, *lane 2*). Complete protection of HER3-ECD$^{I–IV}$ was observed (Fig. 3*B*, *lane 3*) at an approximate 1:1 molar ratio of hrg over HER3-ECD$^{I–IV}$. Fragment 1 has a higher molecular weight in the presence of hrg (Fig. 3*A*, *lane 3*) than in its absence (Fig. 3*A*, *lane 2*), whereas the size of fragment 2 is apparently not affected by the presence of hrg (Fig. 3*A*, *lanes 2–5*). The cleavage that produces fragment 1 is apparently blocked by hrg but produces an additional, smaller fragment, which was not detected in the SDS gel of the digest of HER3-ECD$^{I–IV}$. These data suggest that hrg protects HER3-ECD$^{I–IV}$ from the proteolytic cleavage that generates fragment 1.

Localization of the Cleavage Sites—Taken together, these results suggest that there are at least two cleavage sites, one that is protected by hrg and another that is not. To localize the positions of the cleavage sites, we used N-terminal sequencing and mass spectrometry. Fragment 1 begins at position 51 in the absence of hrg and at position 20 (the first residue in native HER3-ECD$^{I–IV}$) in the presence of hrg (Fig. 4). The N-terminal 31-residue fragment generated from the cleavage following residue 50 was not detected by SDS-PAGE or by mass spectrometry. The corresponding size by mass spectrometry of fragment 1 is 26.7 kDa in the absence of hrg and 30 kDa in the presence (Fig. 4). The difference in mass of fragment 1 in the presence and absence of hrg is 3270 daltons, which corresponds to the predicted size of 3216 daltons, based on the amino acid sequence of the missing fragment (Fig. 4). This suggests that the amino acid residues between positions 20 and 50 of HER3-ECD$^{I–IV}$ are not glycosylated. Based on these results, we conclude that hrg protects HER3-ECD$^{I–IV}$ from proteolysis at position 50.

The cleavage that generates fragment 2 was not blocked by hrg in our assays and is located at position 270. The mass of fragment 2 is 47.0 kDa both in the presence and absence of hrg. The C terminus may contain additional cleavage sites that are not protected by hrg, because there is a missing C-terminal fragment (7.5 kDa) both in the presence and absence of hrg (Fig. 4). However, cleavage of the C terminus could be blocked by an antibody against the V5 epitope tag (Fig. 1*b*).

The cleavage sites on the carboxyl side of Tyr^{50} and Phe^{270} are more typical of chymotryptic rather than tryptic cleavage. This cleavage could be due to chymotrypsin present in the solution purchased from Life Technologies, Inc. However, the identity of the specific protease involved does not affect the finding that hrg protects HER3-ECD$^{I–IV}$ from cleavage at Tyr^{50} but not at Phe^{270}.

Protection Is Due to a Specific Interaction of hrg with HER3-ECD$^{I–IV}$—To show that hrg protection is a result of the specific interaction between hrg and HER3-ECD$^{I–IV}$, we repeated the digestion in the presence of a binding-deficient mutant of hrg (NA_5-hrg) and EGF. NA_5-hrg is deficient in binding due to the fact that the N-terminal residues that confer specific HER3-ECD$^{I–IV}$ binding were mutated to alanine. NA_5-hrg and EGF do not shift the position of HER3-ECD$^{I–IV}$ in a gel mobility shift assay (Fig. 5, *lanes 3* and *4*). The cleavage pattern obtained in the presence of NA_5-hrg and EGF matches that of unprotected HER3-ECD$^{I–IV}$ (Fig. 3*A*, *lanes 4* and *5 versus lane 2*), further confirming that they do not bind hrg. Therefore, the difference in the cleavage pattern in the presence of hrg is due to a specific interaction between hrg and HER3-ECD$^{I–IV}$.

Recombinant HER3-ECD^{I-II} Is Sufficient for Heregulin Binding—To show that a ligand binding site is located within domain I of HER3-ECD$^{I–IV}$, we recombinantly expressed domain

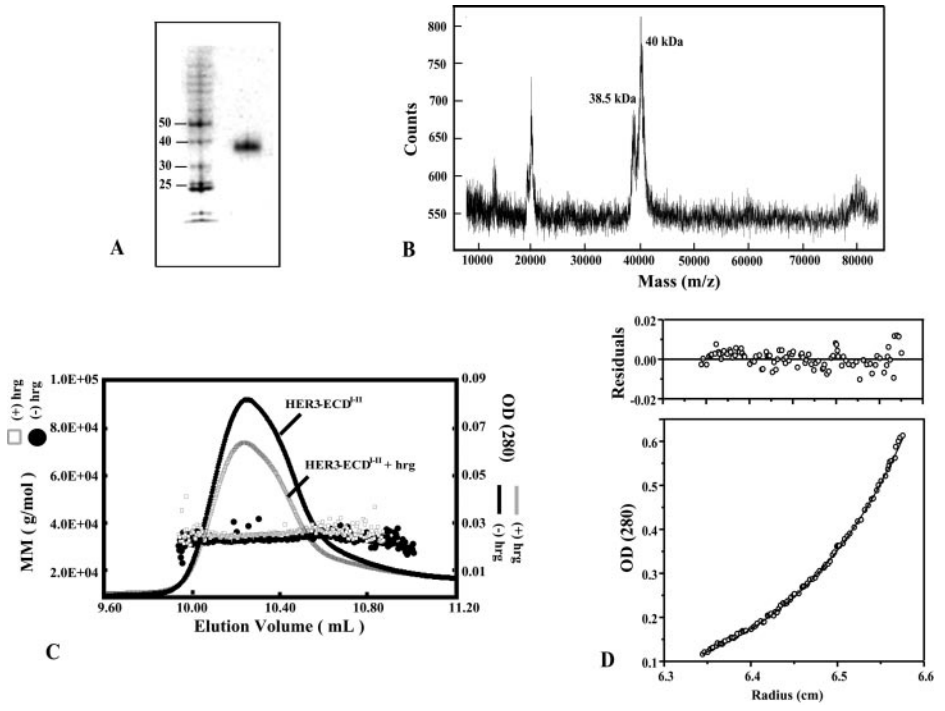

FIG. 6. **Characterization of recombinant HER3-ECD^{I-II} by SDS-PAGE analysis, mass spectrometry, light scattering, and equilibrium centrifugation.** *A*, recombinant HER3-ECD^{I-II} is pure as judged by SDS-PAGE analysis. HER3-ECD^{I-II} was expressed in *Drosophila* S2 cells and purified from the medium. The molecular mass appears to be somewhat less than 40 kDa. *B*, the molecular mass of HER3-ECD^{I-II} is between 38.5 and 40 kDa as determined by MALDI mass spectrometry, compared with a theoretical molecular mass of 37.7 kDa. This suggests that HER3-ECD^{I-II} has a carbohydrate content between 3.3 and 5.7% by weight. *C*, recombinant HER3-ECD^{I-II} is a monomer as determined by size exclusion chromatography followed by multiangle light scattering. Recombinant HER3-ECD^{I-II} eluted in a single peak (*black line*) with a molecular mass of ~34 kDa (S.E. = ± 4%) (*black circles*). The addition of a 1.3-fold molar excess of hrg caused a slight shift in the peak (*gray line*). The shifted peak has a molecular mass of 35 kDa (S.E. = ±3%) (*gray squares*). Recombinant HER3-ECD^{I-II} is a monomer and remains a monomer in the presence of hrg. *D*, recombinant HER3-ECD^{I-II} is a monomer, as determined by ultracentrifugation at three different concentrations and three different speeds. The average molecular mass of HER3-ECD^{I-II} is 35.0 kDa (S.E. = ±0.6%), which corresponds to monomeric HER3-ECD^{I-II}.

I of HER3 alone (HER3-ECD^{I}) as well as domains I and II together (HER3-ECD^{I-II}). Expression of domain I alone resulted in an improperly folded protein because of incorrect disulfide formation (data not shown), so only HER3-ECD^{I-II} could be evaluated for ligand binding. The recombinant form of HER3-ECD^{I-II} (residues 20–329) was expressed in *Drosophila* S2 cells and purified from the medium. The protein was found to be pure by SDS-PAGE analysis with an apparent molecular mass of 40 kDa (Fig. 6*A*). We used MALDI mass spectrometry to estimate the carbohydrate content. The molecular mass of HER3-ECD^{I-II} was found to be between 38.5 and 40 kDa, compared with a theoretical molecular mass of 37.7 kDa (Fig. 6*B*). This suggests that HER3-ECD^{I-II} has a carbohydrate content between 3.3 and 5.7% by weight.

Size exclusion chromatography followed by multiangle light scattering was used to show that recombinant HER3-ECD^{I-II} is a monomer. The concentration of HER3-ECD^{I-II} at the time of light scattering was 1.8 μM. At this concentration, a single peak was observed with a molecular mass of ~34 kDa (S.E. = ±4%) corresponding to monomeric HER3-ECD^{I-II} (Fig. 6*C*). There was a slight shift in the peak upon the addition of a 1.3-fold molar excess of hrg. The shifted peak has an estimated molecular mass of 35 kDa (S.E. = ±3%) (Fig. 6*C*). To confirm that HER3-ECD^{I-II} is a monomer, we used ultracentrifugation at three different concentrations and three different speeds. The estimated average molecular weight of HER3-ECD^{I-II}, using a group analysis of all of the scans, is 35,000 ± 210 daltons (Fig. 6*D*). This is consistent with the expected molecular mass (37.5 kDa) of monomeric HER3-ECD^{I-II}.

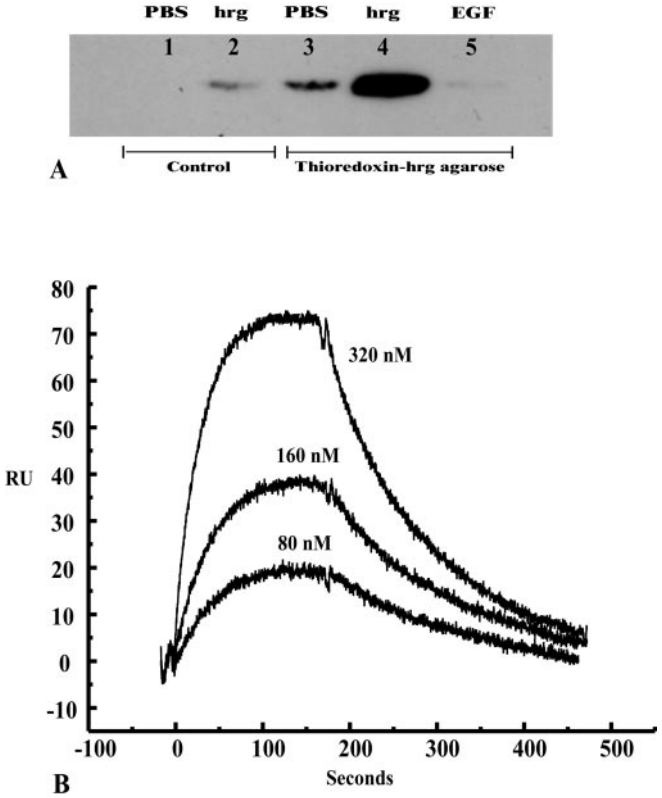

FIG. 7. **Recombinant HER3-ECD^{I-II} binds hrg.** *A*, HER3-ECD^{I-II} was analyzed in a pull-down assay in which S-tagged hrg was immobilized on S-protein resin (*lanes 3–5*) and could be specifically eluted with 1 μM hrg (*lane 4*) but not PBS (*lane 3*) or 1 μM EGF (*lane 5*). The fragment showed little nonspecific binding to S-protein resin without immobilized S-tagged hrg (*lanes 1* and *2*) when eluted with PBS (*lane 1*) or 1 μM hrg (*lane 2*). This shows that domains I and II of HER3-ECD^{I-IV} are involved in hrg binding. *B*, recombinant HER3-ECD^{I-II} has a K_d of 68 nM as determined by SPR (BIAcore). HER3-ECD^{I-II} showed binding to immobilized trx-hrg with a calculated equilibrium dissociation constant of 68 nM using the three different concentrations of HER3-ECD^{I-II} indicated. This shows that HER3-ECD^{I-II} binds hrg.

We used two independent methods to demonstrate direct binding of hrg to HER3-ECD^{I-II}: a pull-down assay and surface plasmon resonance (SPR; BIAcore) analysis. Binding of hrg to HER3-ECD^{I-II} was shown using a pull-down assay under physiological salt conditions. In this analysis, we measured the amount of the V5-tagged HER3-ECD^{I-II} that dissociated from immobilized trx-hrg by the addition of hrg. Using the trx-hrg-coupled S-protein-agarose, HER3-ECD^{I-II} could be eluted with 1 μM hrg (Fig. 7*A*, *lane 4*). In contrast, neither PBS (Fig. 7*A*, *lane 3*) nor EGF (Fig. 7*A*, *lane 5*) was effective in eluting HER3-ECD^{I-II}.

To further confirm that HER3-ECD^{I-II} binds hrg, we analyzed the interaction by SPR (BIAcore). Trx-hrg fusion protein was immobilized on a BIAcore chip for these measurements. SPR measurements using HER3-ECD^{I-II} showed binding to the immobilized trx-hrg with a calculated equilibrium dissociation constant of 68 nM, calculated directly from k_{on} and k_{off} (k_{on} = $(1.07 \pm 0.1) \times 10^5$ M^{-1} s^{-1}; k_{off} = $(7.27 \pm 1) \times 10^{-3}$ s^{-1}) (Fig. 7*b*). This interaction could be inhibited by stoichiometric concentrations of hrg (data not shown). Based on these results, we conclude that HER3-ECD^{I-II} containing domains I and II of HER3 binds hrg.

DISCUSSION

A Ligand Binding Site for Heregulin Is Located in Domain I of HER3—In the current study, we identified two proteolytic sites in HER3-ECD$^{I–IV}$. Cleavage at position 50 is fully protected by hrg binding, whereas position 270 is unprotected. Hrg protection at position 50 is a result of the specific interaction between hrg and HER3-ECD$^{I–IV}$. Only two fragments were detected by SDS-PAGE and mass spectrometry. The N-terminal fragment generated from cleavage at residue 50 could not be detected, but its absence could be due to additional cleavage sites between residues 20 and 50. The cleavage site at position 270 is not protected by hrg, but the fragments generated by this cleavage are held together by disulfide bonds. Hrg protects only one of the cleavage sites in a ligand-specific manner. The extreme C terminus is also sensitive to proteolysis, which could be blocked by an antibody against the V-5 epitope tag but not by hrg.

This protection at position 50 can be explained in two different ways, which include binding of hrg at or near position 50 or indirect protection resulting from a conformational change in HER3-ECD$^{I–IV}$, induced by hrg binding. We could not distinguish between these two possibilities based on the results of the proteolysis experiments; therefore, we expressed domain I and II of HER3-ECD$^{I–IV}$ (HER3-ECD^{I-II}) and assayed it for binding.

HER3-ECD^{I-II} Binds Heregulin—We characterized the association state and binding properties of HER3-ECD^{I-II}. HER3-ECD^{I-II} is a monomer and remains a monomer when hrg is present. This is in contrast to the HER3-ECD$^{I–IV}$ expressed in

TABLE I

The percentage of residue identity between aligned sequences of domains I, II, III, and IV of the EGFR, HER2, HER4, IGF-1R, and HER3-ECD. The IGF-1R structure does not contain an equivalent to domain IV of HER3-ECD.

HER3	Percentage of identity with HER3 domain			
	I	II	III	IV
	%	%	%	%
EGFR	43	48	42	49
HER2	43	48	41	40
HER4	56	67	64	48
IGF-1R	34	32	22	

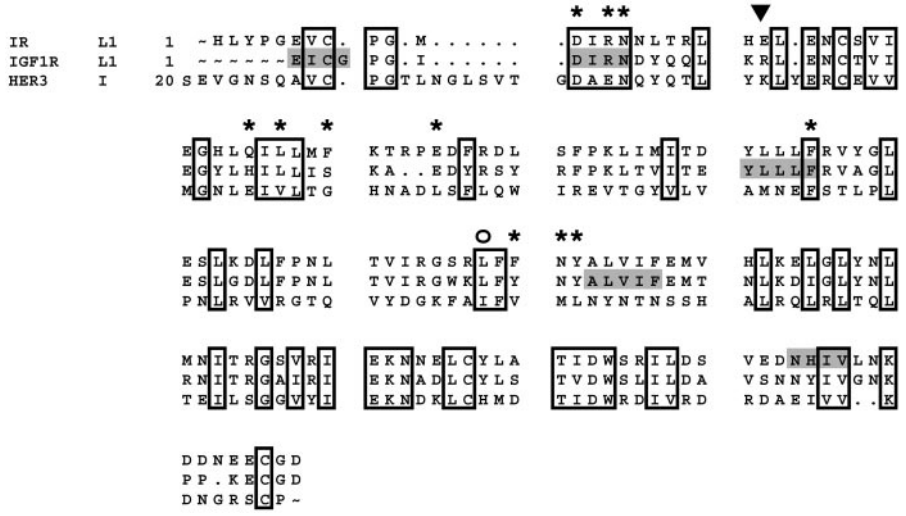

FIG. 8. **Sequence alignment of domain I of HER3-ECD$^{I–IV}$, IR, and IGF-1R indicates the position of the proteolysis site (▼) in domain I of HER3-ECD$^{I–IV}$ relative to mutations (*) that decrease ligand binding in the IR.** A naturally occurring mutation that decreases binding in IR is indicated by an *open circle*. The "hormone binding footprint" in the IGF-1R structure (43) is indicated by *shaded areas* in the sequence. This alignment shows that the proteolysis site HER3-ECD$^{I–IV}$ that is protected by hrg corresponds to the analogous putative ligand-binding region in domain L1 in IGF-1R.

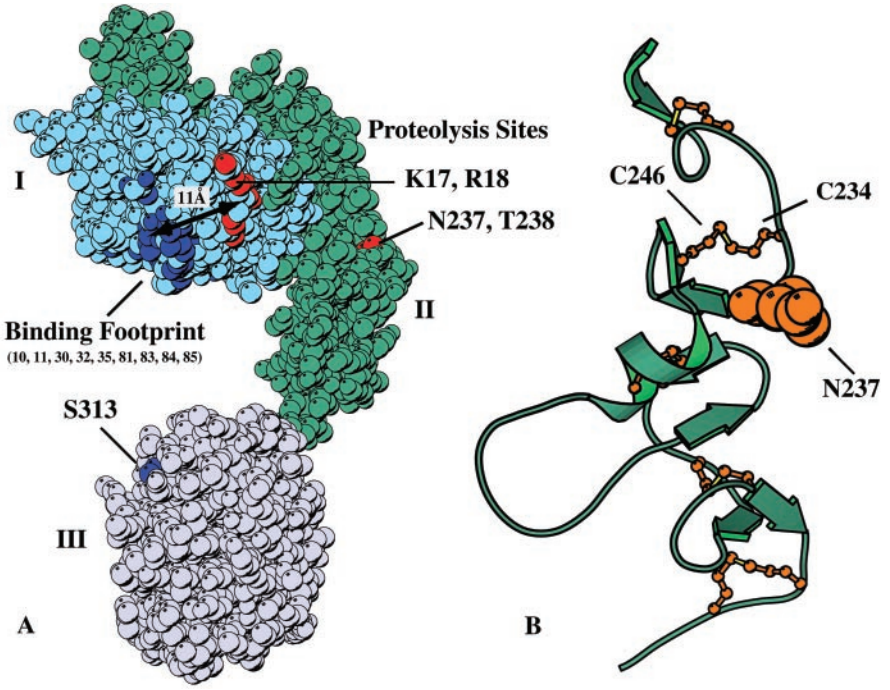

FIG. 9. **Structural similarity of IGF-1R to HER3-ECD$^{I–IV}$.** *A*, space-filling model of domains I and II of the structure of IGF-1R (43) showing the positions of the proteolysis sites (*red*) observed for the HER3-ECD$^{I–IV}$ mapped to the IGF-1R structure. The position of mutations (*dark blue*) that decrease ligand binding in IR are also mapped to a binding footprint in the IGF-1R structure. Domain L1 is *light blue*, and L2 is *lavender* in IGF-1R (domains I and III in HER3-ECD$^{I–IV}$), and domain S1 (domain II in HER3-ECD$^{I–IV}$) is *green*. 1740 Å^2 of accessible surface area in domain L1 are buried by domain S1 in IGF-1R. The cleavage site at position 50 in HER3-ECD$^{I–IV}$ that is protected by hrg (position 18 in IGF-1R) lies on the same face of domain L1 in IGF-1R and is 11 Å away from residue 10 in the binding footprint of IR/IGF-1R. The unprotected cleavage site at position 270 in HER3-ECD$^{I–IV}$ (position 237 in IGF-1R) lies in domain II, is on the opposite side as the binding footprint, and is 40 Å away from the binding footprint. Residue numbers are shown in the binding footprint. The cleavage site that is protected by hrg in HER3-ECD$^{I–IV}$ is near the binding footprint in domain L1 of IGF-1R. *B*, backbone representation of domain II of IGF-1R showing the position of the proteolysis site at position 270 in HER3-ECD$^{I–IV}$ (*red cpk*) (position 237 in IGF-1R) superimposed on the IGF-1R structure. The chain remains connected by a disulfide (*red ball and stick*) when cleavage occurs at position 270. The disulfide bridge connecting fragments I and II of HER3-ECD$^{I–IV}$ is consistent with a structural model based on IR/IGF-1R.

S2 cells in which hrg reverses oligomerization to form a monomer (40). We analyzed direct hrg binding to HER3-ECD^{I-II} by two independent techniques. We qualitatively demonstrated specific binding to hrg binding by a pull-down assay. An equilibrium dissociation constant of 68 nM for hrg binding was calculated by surface plasmon resonance in which the trx-hrg was immobilized. HER3-ECD^{I-II} has 30-fold lower binding affinity than HER3-ECD$^{I–IV}$ (2.3 nM) but a 7-fold greater affinity for its ligand than the extracellular domain of EGFR (500 nM) (25). The absence of domains III and IV could be the reason that HER3-ECD^{I-II} has lower binding affinity. In short, domains I and II of HER3-ECD are sufficient for hrg binding, and the results from proteolysis protection suggest that a ligand binding site is located in domain I.

Limited proteolysis of HER3-ECD$^{I–IV}$ and the expression of HER3-ECD^{I-II} provides evidence that the extent to which different domains of the type I receptor tyrosine kinases (EGFR, HER2, HER3, and HER4) contribute to ligand binding may not be conserved among the members of this EGFR family. Our data suggest that domain I of HER3-ECD$^{I–IV}$ contains a site involved in ligand binding, whereas in EGFR, multiple lines of evidence suggest that the ligand contacts both domain I and III

(20–24) but that domain III alone is sufficient for ligand binding (25). It is noteworthy that the K_d for transforming growth factor binding to the monomeric ECD of EGFR is 500 nM. Domain III of EGFR binds transforming growth factor with a K_d of 1.3 μM. The K_d of HER3-ECD$^{I–IV}$ is 1.9 nM, whereas the K_d for HER3-ECD^{I-II} is 68 nM. Therefore, despite a loss of binding compared with HER3-ECD$^{I–IV}$, HER3-ECD^{I-II} still retains a higher affinity for its ligand than the EGFR ECD. EGFR forms dimers in response to ligand binding (41), whereas HER3-ECD$^{I–IV}$ expressed in S2 cells exists as an oligomer but, following ligand binding, forms a monomer (40). This may be a reflection of the different modes of ligand binding behavior in both receptors. Our data suggest that for HER3-ECD$^{I–IV}$ ligand binding occurs partly in domain I, whereas domain III may also contribute to binding; the relative contribution of domains I and II to binding appears to be shifted in favor of domain I, for HER3.

Structural Homology of IGF-1R to HER3—Further understanding of the activity of type I RTKs has been hindered by the lack of a molecular structure for any member of the family. It has been proposed that the structure of type I RTK ECDs may be similar to the insulin growth factor-1 receptor (IGF-1R) (42, 43). The structure of the first three domains of IGF-1R was solved by x-ray crystallography at 2.6-Å resolution (43). IGF-1R is a type II receptor tyrosine kinase and is a member of the tyrosine kinase superfamily, which includes the type I (EGFR/HER3) subfamily (14). HER3 and IGF-1R have significant sequence identity in portions of the extracellular domain and have a similar domain organization (18, 19). In addition, this equivalence has been proposed based on homology modeling between HER3-ECD$^{I–IV}$ and the IGF-1R structure (42). The IGF-1R structure contains three domains (L1, S1, and L2), which are equivalent to domains I, II, and III in HER3-ECD$^{I–IV}$ (Table I). Domains L1 and L2 are similar in sequence in IGF-1R (25% identity and 41% similarity), as are domains I and III in HER3-ECD$^{I–IV}$ (30% identity and 41% similarity). Domains L1 and L2 also have highly similar structures (43). Alanine-scanning mutagenesis of the insulin receptor, a receptor closely related to IGF-1R, identified four regions in the primary sequence of L1 that were important for ligand binding (44). These regions map to the IGF-1R structure, which reveals a "hormone binding footprint" lying on the face of domain L1 (43). A naturally occurring mutation in the insulin receptor at residue 58 lies within the footprint (45). Other mutations in the insulin receptor also suggest minor contributions in domain L2 (46). A model has been suggested in which ligand binding in the IGF-1R involves domains L1 and L2 (42), which correspond to domains I and III in HER3-ECD$^{I–IV}$.

Our current analysis provides biochemical evidence for the proposed structural similarity of type I (HER3) and II (IGF-1R and IR) RTKs. First, a sequence alignment of domain L1 in the IR and the IGF-1R and domain I in HER3-ECD$^{I–IV}$ was performed (Fig. 8). The cleavage site at position 50, which is protected by hrg corresponds to the putative ligand-binding region in domain L1 in IGF-1R (Fig. 9*A*). Residue 17 in IGF-1R (position 50 in HER3-ECD$^{I–IV}$) lies on the same face as the binding footprint and is 11 Å away from residue 10, which lies within the binding footprint. Second, we expressed HER3-ECD^{I-II}, which binds hrg with a 68 nM dissociation constant, supporting the involvement of domain I in ligand binding. Third, the second proteolysis site in which the fragments are held together by a disulfide bridge at position 270 is located in the cysteine-rich domain II of HER3-ECD$^{I–IV}$ (position 237 in the IGF-1R). Based on the IGF-1R structure, cleavage at this position is expected to result in a disulfide-linked fragment (Fig. 9*B*). Fourth, the large accessible surface area (1782 Å^2) of domain L1 that is buried by domain S1 of IGF-1R and the conserved contacts in this interface in the type 1 RTKs (42) suggest that these domains function as unit. This is consistent with our finding that the expression of domain I of HER3 requires the presence of domain II. Therefore, our results are consistent with the proposal that HER3 has a structure similar to IGF-1R. These data provide further insight into areas in the HER3 receptor critical for heregulin binding.

Acknowledgments—We thank Julian Whitelegge, Parag Mallick, Michael Sawaya, Daniel H. Anderson, and Martin Phillips of UCLA for expert help.

REFERENCES

1. Kraus, M. H., Issing, W., Miki, T., Popescu, N. C., and Aaronson, S. A. (1989) *Proc. Natl. Acad. Sci. U. S. A.* **86,** 9193–9197
2. Ullrich, A., Coussens, L., Hayflick, J. S., Dull, T. J., Gray, A., Tam, A. W., Lee, J., Yarden, Y., Libermann, T. A., Schlessinger, J., Downward, J., Mayes, E. L. V., Whittle, N., Waterfield, M. D., and Seeburg, P. H. (1984) *Nature* **309,** 418–425
3. Schechter, A. L., Hung, M. C., Vaidyanathan, L., Weinberg, R. A., Yang-Feng, T. L., Francke, U., Ullrich, A., and Coussens, L. (1985) *Science* **229,** 976–978
4. Plowman, G. D., Culouscou, J. M., Whitney, G. S., Green, J. M., Carlton, G. W., Foy, L., Neubauer, M. G., and Shoyab, M. (1993) *Proc. Natl. Acad. Sci. U. S. A.* **90,** 1746–1750
5. Sliwkowski, M. X., Schaefer, G., Akita, R. W., Lofgren, J. A., Fitzpatrick, V. D., Nuijens, A., Fendly, B. M., Cerione, R. A., Vandlen, R. L., and Carraway, K. L. (1994) *J. Biol. Chem.* **269,** 14661–14665
6. Fitzpatrick, V. D., Pisacane, P. I., Vandlen, R. L., and Sliwkowski, M. X. (1998) *FEBS Lett.* **431,** 102–106
7. Heldin, C. H. (1995) *Cell* **80,** 213–223
8. Tzahar, E., Pinkas-Kramarski, R., Moyer, J. D., Klapper, L. N., Alroy, I., Levkowitz, G., Shelly, M., Henis, S., Eisenstein, M., Ratzkin, B. J., Sela, M., Andrews, G. C., and Yarden, Y. (1997) *EMBO J.* **16,** 4938–4950
9. Slamon, D. J., Clark, G. M., Wong, S. G., Levin, W. J., Ullrich, A., and McGuire, W. L. (1987) *Science* **235,** 177–182
10. Slamon, D. J., Godolphin, W., Jones, L. A., Holt, J. A., Wong, S. G., Keith, D. E., Levin, W. J., Stuart, S. G., Udove, J., Ullrich, A., and Press, M. F. *(1989) Science* **244,** 707–712
11. Plowman, G. D., Green, J. M., Culouscou, J. M., Carlton, G. W., Rothwell, V. M., and Buckley, S. (1993) *Nature* **366,** 473–475
12. Dougall, W. C., Qian, X., Miller, M. J., and Greene, M. I. (1996) *DNA Cell Biol.* **15,** 31–40
13. Aguilar, Z., Akita, R. W., Finn, R. S., Ramos, B. L., Pegram, M. D., Kabbinavar, F. F., Pietras, R. J., Pisacane, P., Sliwkowski, M. X., and Slamon, D. J. (1999) *Oncogene* **18,** 6050–6062
14. Ullrich, A., and Schlessinger, J. (1990) *Cell* **61,** 203–212
15. Guy, P. M., Platko, J. V., Cantley, L. C., Cerione, R. A., and Carraway, K. L. (1994) *Proc. Natl. Acad. Sci. U. S. A.* **91,** 8132–8136
16. Carraway, K. L., Sliwkowski, M. X., Akita, R., Platko, J. V., Guy, P. M., Nuijens, A., Diamonti, A. J., Vandlen, R. L., Cantley, L. C., and Cerione, R. A. (1994) *J. Biol. Chem.* **269,** 14303–14306
17. Horan, T., Wen, J., Arakawa, T., Liu, N., Brankow, D., Hu, S., Ratzkin, B., and Philo, J. S. (1995) *J. Biol. Chem.* **270,** 24604–24608
18. Yarden, Y., and Ullrich, A. (1988) *Annu. Rev. Biochem.* **57,** 443–478
19. Lax, I., Johnson, A., Howk, R., Sap, J., Bellot, F., Winkler, M., Ullrich, A., Vennstrom, B., Schlessinger, J., and Givol, D. (1988) *Mol. Cell. Biol.* **8,** 1970–1978
20. Lax, I., Bellot, F., Howk, R., Ullrich, A., Givol, D., and Schlessinger, J. (1989) *EMBO J.* **8,** 421–427
21. Lax, I., Fischer, R., Ng, C., Segre, J., Ullrich, A., Givol, D., and Schlessinger, J. (1991) *Cell Regul.* **2,** 337–345
22. Wu, D. G., Wang, L. H., Sato, G. H., West, K. A., Harris, W. R., Crabb, J. W., and Sato, J. D. (1989) *J. Biol. Chem.* **264,** 17469–17475
23. Summerfield, A. E., Hudnall, A. K., Lukas, T. J., Guyer, C. A., and Staros, J. V. (1996) *J. Biol. Chem.* **271,** 19656–19659
24. Wu, D. G., Wang, L. H., Chi, Y., Sato, G. H., and Sato, J. D. (1990) *Proc. Natl. Acad. Sci. U. S. A.* **87,** 3151–3155
25. Kohda, D., Odaka, M., Lax, I., Kawasaki, H., Suzuki, K., Ullrich, A., Schlessinger, J., and Inagaki, F. (1993) *J. Biol. Chem.* **268,** 1976–1981
26. Woltjer, R. L., Lukas, T. J., and Staros, J. V. (1992) *Proc. Natl. Acad. Sci. U. S. A.* **89,** 7801–7805
27. Lemmon, M. A., Bu, Z., Ladbury, J. E., Zhou, M., Pinchasi, D., Lax, I., Engelman, D. M., and Schlessinger, J. (1997) *EMBO J.* **16,** 281–294
28. Huang, G. C., Ouyang, X., and Epstein, R. J. (1998) *Biochem. J.* **331,** 113–119
29. Alimandi, M., Romano, A., Curia, M. C., Muraro, R., Fedi, P., Aaronson, S. A., Di Fiore, P. P., and Kraus, M. H. (1995) *Oncogene* **10,** 1813–1821
30. Kita, Y., Tseng, J., Horan, T., Wen, J., Philo, J., Chang, D., Ratzkin, B., Pacifici, R., Brankow, D., Hu, S., Luo, Y., Wen, D., Arakawa, T., and Nicolson, M. (1996) *Biochem. Biophys. Res. Commun.* **226,** 59–69
31. Landgraf, R., Pegram, M., Slamon, D. J., and Eisenberg, D. (1998) *Biochemistry* **37,** 3220–3228
32. Bidlingmeyer, B. A., Cohen, S. A., and Tarvin, T. L. (1984) *J. Chromatogr.* **336,** 93–104
33. Cohen, S. A., and Strydom, D. J. (1988) *Anal. Biochem.* **174,** 1–16

34. Henikoff, S., and Henikoff, J. G. (1992) *Proc. Natl. Acad. Sci. U. S. A.* **89,** 10915–10919
35. Smith, T., and Waterman, M. (1981) *Adv. Appl. Math.* **2,** 482–489
36. Lee, B., and Richards, F. M. (1971) *J. Mol. Biol.* **55,** 379–400
37. Collaborative Computational Project (1994) *Acta Crystallogr. Sect. D* **50,** 760–763
38. Cohn, E. J., and Edsall, J. T. (1943) in *Proteins, Amino Acids and Peptides as Ions and Dipolar Ions* (Cohn, E. J., and Edsall, J. T., eds) pp. 370–381, Reinhold Publishing Corp., New York
39. Laue, T. M., Shah, B. D., Ridgeway, T. M., and Pelletier, S. L. (1992) in *Analytical Ultracentrifugation in Biochemistry and Polymer Science* (Harding, S. E., Rowe, A. J., and Horton, J. C., eds) pp. 90–125, The Royal Society of Chemistry, Cambridge, United Kingdom
40. Landgraf, R., and Eisenberg, D. (2000) *Biochemistry* **39,** 8503–8511
41. Hurwitz, D. R., Emanuel, S. L., Nathan, M. H., Sarver, N., Ullrich, A., Felder, S., Lax, I., and Schlessinger, J. (1991) *J. Biol. Chem.* **266,** 22035–22043
42. Jorissen, R. N., Epa, V. C., Treutlein, H. R., Garrett, T. P. J., Ward, C. W., and Burgess, A. W. (2000) *Protein Sci.* **9,** 310–324
43. Garrett, T. P., McKern, N. M., Lou, M., Frenkel, M. J., Bentley, J. D., Lovrecz, G. O., Elleman, T. C., Cosgrove, L. J., and Ward, C. W. (1998) *Nature* **394,** 395–399
44. Williams, P. F., Mynarcik, D. C., Yu, G. Q., and Whittaker, J. (1995) *J. Biol. Chem.* **270,** 3012–3016
45. van der Vorm, E. R., van der Zon, G. C., Moller, W., Krans, H. M., Lindhout, D., and Maassen, J. A. (1992) *J. Biol. Chem.* **267,** 66–71
46. Nakae, J., Morioka, H., Ohtsuka, E., and Fujieda, K. (1995) *J. Biol. Chem.* **270,** 22017–22022